Journal of Coastal Research	21	6	1173–1177	West Palm Beach, Florida	November 2005

Artificial Neural Network Classification of Sand in all Visible Submarine and Subaerial Regions of a Digital Image

Christopher L. Conger, Charles H. Fletcher, and Matthew Barbee

Department of Geology and Geophysics
School of Ocean and Earth Science and Technology
University of Hawaii
1680 East West Road
Honolulu, HI 96822, U.S.A.
conger@hawaii.edu

ABSTRACT

CONGER, C.L.; FLETCHER, C.H., and BARBEE, M., 2005. Artificial Neural Network Classification of Sand in All Visible Submarine and Subaerial Regions of a Digital Image. *Journal of Coastal Research,* 21(6), 1173–1177. West Palm Beach (Florida), ISSN 0749-0208.

Factors controlling the distribution of shelf sand as a resource, a component of reef ecosystems, and a dynamic substrate are poorly understood. An initial step in understanding sand accumulation in each of these roles is to identify its areal extent and change through time. Digitized aerial photographs and digital images provide common, inexpensive data sets that are generally underutilized for the purpose of marine substrate classification. Here we use only two bands, blue and green (470 and 550 nm), to demonstrate the utility of simple aerial photography in classifying marine substrate. Although these two are acquired from a hyperspectral data set, they represent blue and green in an RGB image such as commonly available in digitized aerial photographs. We add as a third band the second eigenchannel of a principal components analysis of these bands. Using an artificial neural network classification model, we identify submarine and subaerial sandy substrate in a digital image of a detached reef island in the Red Sea, Gezirat Siyul, Egypt. With careful selection of training and test groups, using small percentages of the total classified image, we create an efficient and accurate classification model. The model, trained to identify two classes, "sand" and "other than sand," produces a classified image that provides sand locations and approximate areal coverage. Confusion matrices for both training and testing groups have user's accuracies in the 90 percentiles, indicating accurate pixel classification.

ADDITIONAL INDEX WORDS: *Egypt, neural network testing, remote sensing, image analysis, PCI Geomatics, carbonate sand, remote sensing, coastal geology, shelf sand, reefs, Red Sea.*

INTRODUCTION

Shallow marine sand is an important resource, an integral component of the reef system, and a highly dynamic substrate. Currently there is a dearth of information concerning sand in each of these roles. As a result, our understanding of shallow marine sand changes through time and our ability to manage sand as a resource are not optimal. Inexpensive, efficient, and accurate image products that track sand spatial distribution and temporal variability are significant assets for improving understanding of sand dynamics.

Many available remotely sensed data sets, like aerial photographs, do not provide the high spectral resolution needed to separate multiple information classes. However, when identifying the monotonic signature of sand, multiple classes are not necessary. Most substrate classifications of digital imagery rely on ground truth data to generate training classes or a library of identified spectral returns or both. These methods require analysts to collect field data or acquire hyper/multispectral imagery or both. Here, we develop a simple method to classify shallow sandy substrate without the aid of ground truth data, a spectral library, or hyper/multispectral imagery. The goal of this analysis was to minimize cost while remaining entirely remote during analysis of the image.

To achieve these goals we use analyst-derived training classes to define an artificial neural network (ANN) that models a three-band data set comprising blue (470 nm), green (550 nm), and a third band consisting of the second eigenchannel of a principal components analysis of the blue and green wavelengths. Terrestrial image analysts have successfully used ANN classification programs in various environments (EGMONT-PETERSON *et al.,* 2002; MOHANTY and MAJUMDAR, 1996). They have high success rates with models that apply basic classifications to the digital image (SERPICO *et al.,* 1996). It is our intent to generate an ANN that queries for the simple presence or absence of sand, thus refining for marine application, techniques previously used in terrestrial settings.

STUDY SITE

Gezirat Siyul is a roughly triangular island formed by a shore-detached reef platform along the Egyptian coast of the

DOI:10.2112/03-0099.1 received 5 September 2003; accepted in revision 7 April 2004.

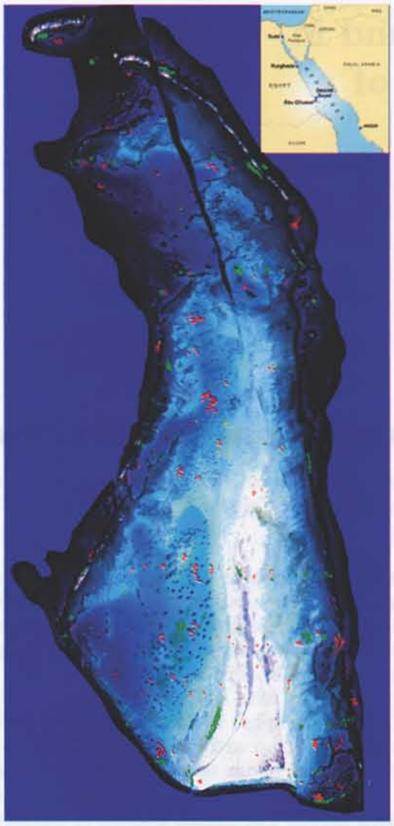

Figure 1. Original digital image of Gezirat Siyul, Egypt, with location in the Red Sea as an inset image. Red pixels are sand training pixels. Green pixels are other than sand training pixels. Yellow pixels are sand test pixels. Magenta pixels are other than sand test pixels. Blue pixels around the outside are masked out of the classification process. A data gap in the flight lines trends 161° from the northern edge of the image.

Red Sea. The island has limited vegetation and is almost exclusively sand in composition. The southern, eastern, and western reef crests are ~700 m, ~850 m, and 1020-m in length, respectively. A shallow sand and gravel bar extends north of the island. A wide-fringing reef and large sand field extend seaward from east, west, and north sides of the island but vary in morphology (Fig. 1).

METHODS

Initial Data

Hyperspectral data of Gezirat Siyul and surrounding waters were acquired with 1-m pixel resolution on 3 April 2000. The data were processed in a four-band format containing georectified, eight-bit, pixel interleaved information for bands at 470, 550, 608, and 850 nm.

We utilized the 470- and the 550-nm bands from the processed image data. Bands at both 608 and 850 nm did not register returns for any significant depth below sea level and consequently were not included in our analysis. To begin identifying differences in bottom type, we applied a principal components analysis and used the second eigenchannel from these two bands. The transformed data highlights features not evident in the original image (RICHARDS and JIA, 1999). The first eigenchannel was dominated by changes in bathymetry, while variation in the second eigenchannel was more closely related to diversity in the bottom types, though not accurately enough to classify the image. For input values for the neural network, we used three eight-bit channels: 470 nm, 550 nm, and the second eigenchannel.

Artificial Neural Network

We use the ANN provided by PCI Geomatics in the Xpace software. ANNs are computer replications of biological systems. Input data are interlinked to a set of multiple, simple decision tools (neurons) that conduct basic operations on the data before passing them forward to the next set of neurons. PCI's ANN is a back-propagation network that utilizes the Generalized Delta Rule for learning. This is a type of multilayer feed-forward network that adjusts the connection weights between each layer during the back-propagation process (PCI GEOMATICS STAFF, 2003).

Training

We specified pixels within training classes using a polygon seeding tool that starts from a single pixel and moves outward choosing similar pixels. We chose initial seed pixels by their color and location within the image. This process requires an experienced marine geologist capable of identifying sandy substrate in remotely sensed images of submarine environments without *a priori* knowledge. Figure 1 shows the "sand" training pixels as red areas and the "other than sand" training areas as green pixels. Tolerance within the seeding program can be adjusted between levels 1 and 50, from most stringent to most relaxed, respectively. We chose to use values between one and six to limit the cluster size of the training pixels and ensure those pixels chosen were similar to the original seed pixel. We also chose to collect small clusters of pixels from spatially well-distributed locations across the visible sea floor, the island, and exposed portions of the reef. The sand training class comprised 61,323 pixels, or 0.67% of the classified image. The other than sand training class comprised 51,120 pixels, or 0.56% of the classified image.

Individual training pixels are fed through the network during the training portion of the program. In creating the network, we chose the number of layers in the ANN, the cutoff tolerances for individual pixel errors, total normalized error, maximum number of iterations, and the speed or learning and momentum rates at which the connections between the layers are adjusted. We used three layers for the network. Pixel values for each channel constitute the input layer. Initial discrimination and conversion to a new coordinate system occur in the hidden layer. Final discrimination and class labeling occur in the output layer.

After all training pixels have passed through the network, the program conducts an error analysis for all individual pixels and for each training group. If errors are outside the predetermined cutoff limits and the maximum number of learning cycles has not been reached, then the total normalized error for all training pixels is used by the Generalized Delta

Rule to reweight each connection during back-propagation (Clothiaux and Bachmann, 1994). Then the next learning cycle is begun.

We used 0.005 as our maximum normalized total error, 0.001 as our maximum individual error, and 1000 as our maximum number of learning cycles. The amount of reweighting, or the magnitude of corrections, is controlled by both the learning rate and the momentum rate. Learning rate, between 0.1 and 1.0, controls how quickly the network stabilizes, with high rates possibly converging early. Momentum rate, between 0.1 and 1.0, controls the step size of corrections, with high rates possibly overstepping and preventing convergence. We chose to use moderate values of 0.6 and 0.5, respectively, which increased both computing time and accuracy.

Network training ends when one of the three preset cutoff limits is reached. If the process is stopped because it reaches the maximum number of learning cycles, then the analyst needs to either choose new training pixels (because the classes are not distinct enough for the network to separate them) or choose higher tolerances for individual error and total normalized error.

We trained our network to ask two simple questions: "Is this or is this not sand?" and "Is this or is this not something other than sand?" By choosing one training class to identify all other bottom types, we have simplified our query and allowed the network to focus on a simple discrimination between sand pixels and all other pixels. Once the network has been trained to a sufficiently low error, as seen in Table 1, the next important step is to ensure that low error cutoffs are not the result of local error minima instead of a global error minimum (Hewitson and Crane, 1994). One method to check the model's global accuracy is to compare its results against test pixel sets.

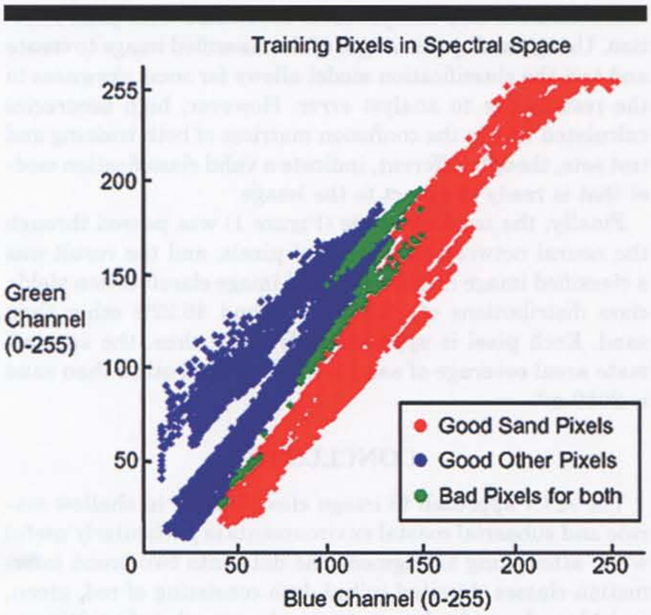

Figure 2. Spectral plot of all training pixels. Red, blue, and green are sand, other than sand, and misclassified training pixels, respectively.

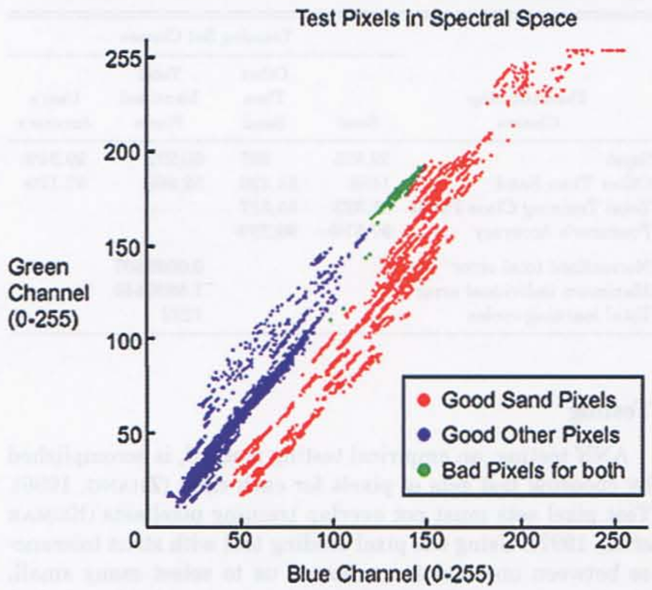

Figure 3. Spectral plot of all test pixels. Red, blue, and green are sand, other than sand, and misclassified test pixels, respectively.

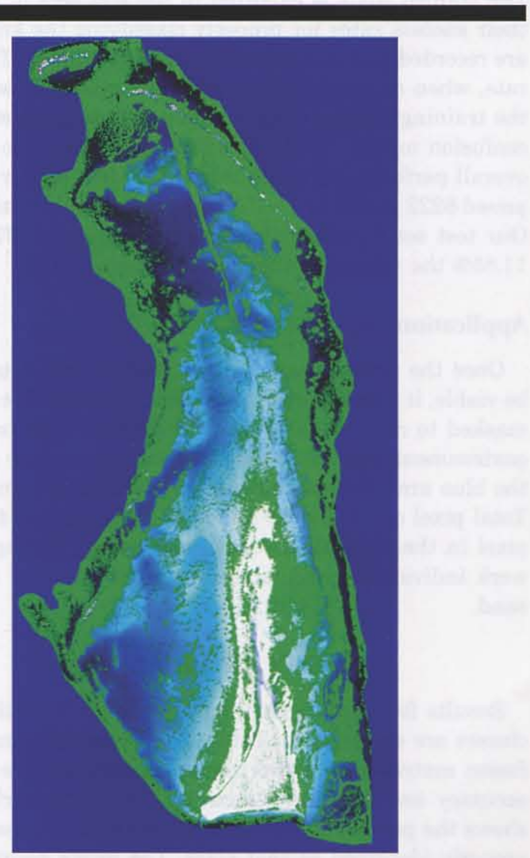

Figure 4. Classified image. Classified sand pixels are visible. Green pixels are classified as other than sand. Blue pixels around the outside are masked out of the classification process.

Table 1. *Confusion matrix for the training pixels.*

Thematic Map Classes	Training Set Classes: Sand	Other Than Sand	Total Identified Pixels	User's Accuracy
Sand	59,835	397	60,232	99.34%
Other Than Sand	1488	51,120	52,608	97.17%
Total Training Class Pixels	61,323	51,517		
Producer's Accuracy	97.57%	99.23%		
Normalized total error			0.0039607	
Maximum individual error			1.6830440	
Total learning cycles			1222	

Table 2. *Confusion matrix for the test pixels.*

Thematic Map Classes	Test Set Classes: Sand	Other Than Sand	Total Identified Pixels	User's Accuracy
Sand	5881	4	5885	99.93%
Other Than Sand	341	6103	6444	94.71%
Total Testing Class Pixels	6222	6107		
Producer's Accuracy	94.52%	99.93%		

Testing

ANN testing, an empirical testing method, is accomplished by choosing test sets of pixels for each class (ZHANG, 1996). Test pixel sets must not overlap training pixel sets (KUMAR *et al.,* 1997). Using the pixel seeding tool with strict tolerances between one and four allowed us to select many small, similar packages of pixels for testing. Again, initial seed pixel selection requires an experienced marine geologist, as they are chosen according to color and location within the image. Figure 1 shows the test pixels. Yellow areas are sand test pixels, and magenta areas are other than sand test pixels. The trained ANN is exported to the test sets of pixels, and their success rates for properly classifying the known pixels are recorded within a confusion matrix (Table 2). This success rate, when combined with both the statistics produced from the training process error analysis and an analyst-computed confusion matrix (Table 1), allows the analyst to assess the overall performance of the ANN. Our test set for sand comprised 6222 pixels, or 10.15% the volume of the training class. Our test set for other than sand comprised 6107 pixels, or 11.85% the volume of the training class.

Application

Once the network was trained, tested, and determined to be viable, it was exported to the entire image. The image was masked to remove all areas were the sea floor or subaerial environment was not visible. Figure 1 shows the mask; it is the blue area around the outside of the island and its reefs. Total pixel count for the classified image is 9,174,405. Each pixel in the unmasked region was passed through the network individually and labeled as either sand or other than sand.

RESULTS AND DISCUSSION

Results for creating the neural network from the training classes are displayed in Table 1 as a confusion matrix. Confusion matrices have two important outputs: the producer's accuracy and the user's accuracy. The producer's accuracy shows the percent of the training pixels for a class that were properly identified as that class. The user's accuracy shows the percent of pixels identified as a class that was actually from that training class. The user's accuracy is most useful because it is a way of quantifying how well the network identified the pixels it was presented (RICHARDS and JIA, 1999). User's accuracy for the sand at 99.34% and other than sand at 97.17% was sufficient to warrant testing the network.

The network required 1222 learning cycles to fall beneath the limit for normalized total error. The tolerance was increased from 0.001 to 0.005 after the first 1000 learning cycles. The final normalized total error was 0.0039607, and the final maximum individual error was 1.6830440, as seen in Table 1. Analysis of incorrectly identified pixels in each class indicates that margins between bright, hard-bottom substrate and sand, in shallow water, are repeatedly misclassified as hard bottom. Additionally, dark material, possibly rubble or algae-covered sand, within sand fields are repeatedly misclassified as sand. Pixels for each training class are displayed in blue *vs.* green spectral space in Figure 2. The green pixels, those misclassified in both classes, are overlapping in the margin between the two classes.

Results from sending test pixels through the network are displayed in Table 2 as a confusion matrix. Pixels for each test class are displayed in blue *vs.* green spectral space in Figure 3. There are differences in the accuracies reported for the training and test statistics. We believe these differences are the result of both normal variation of the image's spectral characteristics and analyst error associated with pixel selection. Using small percentages of the classified image to create and test the classification model allows for some skewness to the results due to analyst error. However, high accuracies calculated within the confusion matrices of both training and test sets, though different, indicate a valid classification model that is ready to export to the image.

Finally, the masked image (Figure 1) was passed through the neural network as individual pixels, and the result was a classified image (Figure 4). Final image classification yields class distributions of 53.78% sand and 46.22% other than sand. Each pixel is approximately 1 m^2; thus, the approximate areal coverage of sand is 2221 m^2, and other than sand is 2059 m^2.

CONCLUSION

The ANN approach to image classification in shallow marine and subaerial coastal environments is particularly useful when attempting to segment the data into two broad information classes. Limited initial data consisting of red, green, and blue channels does not provide enough information to compare with hyper/multispectral signature libraries and requires some preclassification processing to assist in discrimination by a supervised classification model. We found principal components analysis to be a useful preprocessing tool, with the first eigenchannel displaying variation resulting from bathymetric changes and the second eigenchannel displaying variation associated with substrate change. Including subaerial sand in our sand class and subaerial nonsand features in our other than sand class extended the range of our neural network from submarine through subaerial environments.

There is inherent difficulty in creating a classification model that functions in both environments simultaneously while producing accurate results. Training and test pixels are chosen by the analyst without the aid of ground truth data; thus, there exists a potential error for incorrect class identification and pixel labeling. Care should be taken when choosing the amount and location of both training and test pixels. Training groups that are too large, that provide inadequate spatial coverage across the image, or both can lead to a skewed network favoring one section of the spectral information.

Use of a seeding tool with strict control on tolerance settings is critical for selecting viable training and test groups. Learning and momentum rates have a significant impact on network accuracy; thus, increased computing time resulting from lower rates is considered a worthwhile investment in network accuracy. Testing is an important step for validating that the error results were a product not of local error minima but rather of the global error minimum and are representative of the entire image and not just the training pixels.

ANN classification techniques in this application will require new models for each data set, or digital image. Our study indicates that ANN classification, when applied to a single image, is an effective and efficient sand identification tool. Figure 4 shows the classified image with the areas chosen as sand left visible. However, because of the robust nature of this model when applied to simple distinctions, it may be used to classify several different data sets that cover a continuous area of both submarine and subaerial environments. Testing this application should be the next step in identifying an efficient and accurate method for initial sand resource identification from spectrally limited but readily available digitized aerial photographs and digital imagery.

ACKNOWLEDGMENTS

We would like to thank the Office of Naval Research, Geology and Geophysics Program, for support of the principal author in the form of a graduate fellowship paid through award N00014-02-1-0799. Additionally, we would like to thank the United States Geological Survey, the Khaled Bin Sultan Living Oceans Foundation, and Hyperspectral Data International for their generous help in providing data and resources. Finally, we would like to thank Dr. Mathew McGranaghan from the Geography Department at the University of Hawaii for his tireless assistance and invaluable explanations, both of which helped develop and understand the processes applied in this study.

LITERATURE CITED

CLOTHIAUX, E.E. and BACHMANN, C.M., 1994. Neural networks and their applications. *In:* HEWITSON, B.C. and CRANE, R.G. (eds.), *Neural Nets: Applications in Geography.* Amsterdam: Kluwer Academic Publishers, pp. 11–52.

EGMONT-PETERSON, M.; DE RIDDER, D., and HANDELS, H., 2002. Image processing with neural networks—a review. *Pattern Recognition,* 35, 2279–2301.

HEWITSON, B.C. and CRANE, R.G., 1994. Looks and uses. *In:* HEWITSON, B.C. and CRANE, R.G. (eds.), *Neural Nets: Applications in Geography.* Amsterdam: Kluwer Academic Publishers, pp. 1–9.

KUMAR, A.S.; BASU, S.K., and MAJUMDAR, K.L., 1997. Robust classification of multispectral data using multiple neural networks and fuzzy integral. *IEEE Transactions on Geosciences and Remote Sensing,* 35(3), 787–790.

MOHANTY, K.K. and MAJUMDAR, T.J., 1996. An artificial neural network (ANN) based software package for classification of remotely sensed data. *Computers and Geosciences,* 22(1), 81–87.

PCI GEOMATICS STAFF, 2003. Neural network classification. *Xpace User's Help Guide.* Richmond Hill, Ontario, Canada: PCI Geomatics.

RICHARDS, J.A. and JIA, X., 1999. *Remote Sensing Digital Images.* New York: Springer. 363p.

SERPICO, S.B.; BRUZZONE, L., and ROLI, F., 1996. An experimental comparison of neural and statistical non-parametric algorithms for supervised classification of remote-sensing images. *Pattern Recognition Letters,* 17, 1331–1341.

ZHANG, Y.J., 1996. A survey on evaluation methods for image segmentation. *Pattern Recognition,* 29(8), 1335–1346.